
MEIT: Multi-Modal Electrocardiogram Instruction Tuning on Large Language Models for Report Generation

Zhongwei Wan^{1*} Che Liu^{3*} Xin Wang¹ Chaofan Tao⁵ Hui Shen¹
Zhenwu Peng⁴ Jie Fu⁶ Rossella Arcucci³ Huaxiu Yao^{2†} Mi Zhang^{1†}

¹The Ohio State University ²University of North Carolina at Chapel Hill

³Imperial College London ⁴King's College London ⁵HKU ⁶HKUST

Code: <https://github.com/AIoT-MLSys-Lab/MEIT>.

Correspondence to wan.512@osu.edu mizhang.1@osu.edu

Abstract

Electrocardiogram (ECG) is the primary non-invasive diagnostic tool for monitoring cardiac conditions and is crucial in assisting clinicians. Recent studies have concentrated on classifying cardiac conditions using ECG data but have overlooked ECG report generation, which is time-consuming and requires clinical expertise. To automate ECG report generation and ensure its versatility, we propose the **Multimodal ECG Instruction Tuning (MEIT)** framework, the *first* attempt to tackle ECG report generation with LLMs and multimodal instructions. To facilitate future research, we establish a benchmark to evaluate MEIT with various LLMs backbones across two large-scale ECG datasets. Our approach uniquely aligns the representations of the ECG signal and the report, and we conduct extensive experiments to benchmark MEIT with nine open-source LLMs using more than 800,000 ECG reports. MEIT's results underscore the superior performance of instruction-tuned LLMs, showcasing their proficiency in *quality report generation*, *zero-shot capabilities*, and *resilience to signal perturbation*. These findings emphasize the efficacy of our **MEIT** framework and its potential for real-world clinical application.

1 Introduction

Diagnosing heart diseases is of paramount importance, requiring the analysis of multimodal data sources, which include electrocardiogram (ECG) recordings and clinical reports. Cardiologists read and interpret these ECG recordings to manually generate comprehensive ECG reports for heart disease diagnosis, which is a complex and time-consuming process. Recently, AI models have been developed to facilitate ECG data analysis for the task of classification [1–4]. Despite these efforts, the automatic generation of reports from ECG recordings still needs to be explored. Unlike other AI-empowered medical report generation applications (e.g., radiology reports), the primary challenge for ECG report generation stems from the distinct nature of ECG content. ECG reports, often comprising brief phrases that summarize signal patterns, contrast with detailed anatomical descriptions in radiology reports. The difference in the content and semantic interpretation between imaging and ECG data complicates the direct application of radiology-focused methods to ECG reports. Furthermore, there is still a lack of comprehensive benchmarks for evaluating the performance of ECG report generation.

* Core contribution.

†† Core advising.

To tackle these challenges, we introduce MEIT, a **Multimodal ECG Instruction Tuning** framework that extends the capabilities of LLMs in the cardiology context to generate ECG reports using ECG recordings and human instructions. Inspired by the versatility of LLMs [5–9] in handling diverse language tasks simultaneously, we develop a specialized instruction tuning process for ECG report generation. MEIT aligns human instructions with ECG recordings, enabling LLMs to generate professional-grade reports and exhibit zero-shot report generation capabilities under domain transfer scenarios across various continents and data collection devices. Specifically, leveraging publicly available ECG datasets, we construct a multimodal instruction dataset including ECG records, human instructions, and paired reports. Then, we propose an effective and efficient attention-based fusion method to integrate ECG and text representations in the latent space. This enables LLMs to understand ECG signals for report generation without introducing additional training parameters in the attention layer. In addition to the ECG report generation approach, we introduce a comprehensive benchmark for ECG report generation evaluation, utilizing two datasets with 20K and 800K ECG-report pairs, respectively, across three evaluation tasks: report generation quality, zero-shot learning across datasets, and robustness analysis in the face of ECG signal perturbation. Utilizing the ECG report evaluation benchmark, we assess the proposed approach across nine open-source LLMs. The results demonstrate (1) the superior performance of MEIT in ECG report generation and the effective learning and alignment of ECG representations; (2) the effective transferability of LLMs under the MEIT framework in domain transfer scenarios.

To summarize, our primary contribution is the MELT framework, a novel approach to automating ECG report generation and evaluation based on LLMs. This framework incorporates a lightweight, attention-based fusion module across various LLM models. Furthermore, we design a new benchmark for ECG report generation, which contains three evaluation tasks. Our evaluations showcase the enhanced capabilities of instruction-tuned LLMs in generating ECG reports, highlighting the transferability in zero-shot tests and robustness against data perturbations. MEIT paves the way for future advances in automated ECG report generation and methodological innovations in integrating biomedical signals into LLMs.

2 Preliminaries

Electrocardiogram (ECG) measures the electrical activity of an individual’s heart over time. An ECG recording typically contains a 12-lead multivariate time series, which acts as a 12-dimensional sequence of embeddings. The ECG signal offers a comprehensive view, encompassing both spatial and temporal aspects of cardiac function. ECG leads can be categorized into six limb leads (i.e., I, II, III, aVR, aVL, and aVF) to monitor arms and legs, providing frontal plane views, and six precordial leads (i.e., V1, V2, V3, V4, V5, and V6) to monitor chest, showing horizontal plane views. We denote an ECG recording as $\mathbf{X}_e \in \mathcal{R}^{M \times T}$, where M represents the number of leads, and T is signal length. Each ECG recording is associated with an ECG report \mathbf{X}_t for description. Thus, we denote each ECG pair as $\{\mathbf{X}_e, \mathbf{X}_t\}$. More details on visualization can be found in the appendix A.5.

3 MEIT

Figure 1 illustrates the proposed MEIT framework. We begin by describing the curation process for ECG instruction data. We then delve into the architecture of the multimodal LLM designed for ECG report generation. Lastly, we describe the approach to generating ECG reports with instruction tuning.

3.1 ECG Instruction Data Curation

Given an ECG signal \mathbf{X}_e , our goal during inference is to generate an ECG report using an instruction prompt. For instance, the prompt can be “*Given the ECG signal embeddings, please help me generate an accurate description for this ECG signal embeddings:* ”. To achieve this goal, during the training phase, we aim to create instruction tuning data to generate a response $\hat{\mathbf{X}}_t$ that aligns semantically with the ground truth \mathbf{X}_t . In addition, since we cannot predict the exact instruction prompt that users will use, we need to ensure that our report generation process is robust enough to handle different prompts. To address this challenge, we manually design some prompt samples, then utilize GPT-4 [5] to generate a set of prompts by rephrasing, as shown in Figure 1. Then, we randomly select one

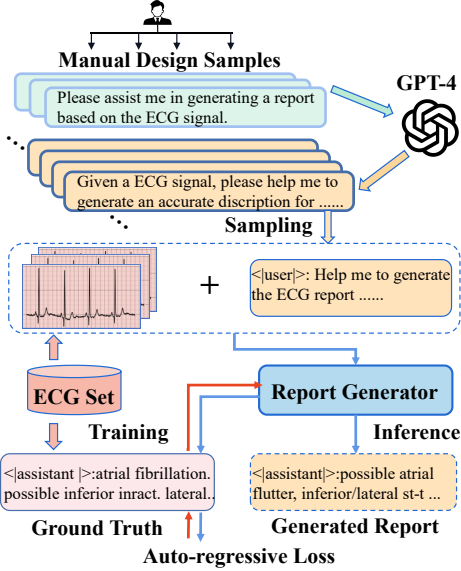


Figure 1: Illustration of the proposed MEIT framework, including ECG instruction data curation, instruction tuning on auto-regressive objective, and inference to get the generated report.

instruction prompt \mathbf{X}_p from the prompt set and create a general instruction-following template: $\langle \text{user} \rangle: \{\mathbf{X}_p, \mathbf{X}_e\} \langle \text{assistant} \rangle: \{\mathbf{X}_t\} \langle /s \rangle$, where $\langle \text{user} \rangle$ and $\langle \text{assistant} \rangle$ are added special tokens for tokenizer, $\langle /s \rangle$ is a stop sign for each response. This approach ensures that the generated response conveys the same meaning as the ground truth and remains adaptable to different instruction prompts. Following this strategy, we construct the ECG instruction data using a MIMIC-IV-ECG [10] dataset that contains 80K annotated data and a 20K dataset PTB-XL [11]. The ECG instruction data samples are shown in Appendix A.5.

3.2 ECG Report Generation Model

In MEIT, the multimodal ECG report generation model decodes ECG signals end-to-end to generate ECG reports. The architecture is illustrated in Figure 2. Specifically, the report generation model directly encodes an entire ECG-signal $\mathbf{X}_e \in \mathcal{R}^{M \times T}$ into latent embeddings and integrate it with the language embeddings with modality alignment, and then autoregressively generate the ECG report. Next, we detail each component of the report generation model.

ECG Encoder. Since the ECG signal is of high resolution in the temporal domain, it is vital to efficiently extract temporal features per lead before interaction with semantic embeddings inside the LLM backbone. Our default ECG encoder $\mathcal{F}_e(\cdot)$ consists of temporal convolution blocks to encode each ECG signal into embeddings. Specifically, each temporal convolution block comprises several 1-D convolution layers, batch normalization layers, and ReLU activation layers, followed by average pooling. To align the output dimension with the head dimension of LLM backbone $\mathcal{F}_l(\cdot)$, we employ a non-linear projection layer $\mathcal{P}_e(\cdot)$ to obtain the ECG embeddings:

$$\mathbf{H}_e = \mathcal{P}_e(\mathcal{F}_e(\mathbf{X}_e)), \quad (1)$$

where $\mathbf{H}_e \in \mathcal{R}^{D_h}$, D_h has the same dimension as the multi-head attention layers of LLMs. Note that our default ECG encoder is lightweight and is able to learn temporal patterns of signals without a long training period. More details about ECG Encoder are illustrated in Appendix A.3.

ECG Modality Alignment. We introduce an ECG modality alignment strategy to guide the LLMs in aligning ECG signal data with corresponding textual outputs. This approach is detailed in Figure 2. Specifically, given the ECG embeddings \mathbf{H}_e , the alignment strategy incorporates \mathbf{H}_e with the current hidden state \mathbf{H}_i^l generated from previous $i - 1$ -th layer of the LLM backbone $\mathcal{F}_l(\cdot)$ for next-token

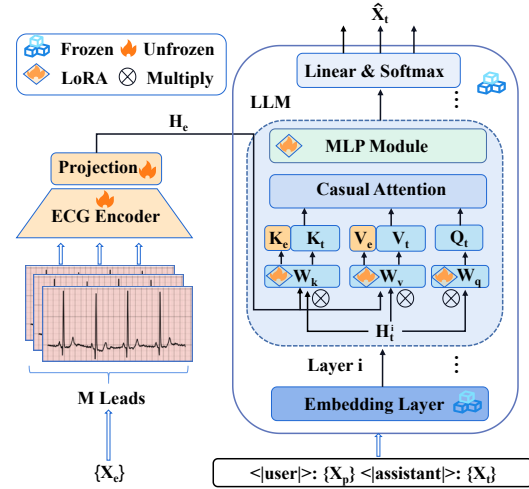


Figure 2: Illustration of model architecture for ECG Report Generation. K_e and V_e refer to linear projection of \mathbf{H}_e by multiplying shared \mathbf{W}_k and \mathbf{W}_v in the attention layer.

prediction task. Here \mathbf{H}_t^i is defined as:

$$\mathbf{H}_t^i = \mathcal{F}_l^{i-1}([\mathbf{X}_p, \mathbf{X}_t]), \quad (2)$$

where i is the current layer index. Different from gated-attention fusion in Flamingo [12], Memorizing Transformer [13], and G-MAP [14], or Q-former in BLIP-2 [15] that require the additional trainable parameters and design complex modules for two-stage training, we propose a simple yet effective concatenated-fusion method that directly injects the ECG embeddings with language context in the causal-attention (C-Attn) of the models. In our approach, each attention layer combines \mathbf{H}_e , generated from the ECG encoder and projector as a prefix condition, with \mathbf{H}_t^i , derived from the preceding layer. The fusion process is as follows:

$$\text{C-Attn}(\mathbf{H}_e, \mathbf{H}_t^i) = [\text{head}_1, \dots, \text{head}_k] \mathbf{W}_o, \quad (3)$$

where k represents the number of attention heads, and \mathbf{W}_o , a matrix in $\mathcal{R}^{kD_h \times D_m}$, serves as the projection matrix with D_m denoting the hidden size of the LLM backbone. We replicate \mathbf{H}_e for each head k times, merging the ECG and language features in the sequence dimension. This is achieved through a shared projection of keys and values for each pattern. The fusion is then articulated as:

$$\mathbf{K}_{m,j} = [\mathbf{K}_{e,j}, \mathbf{K}_{t,j}]^\top, \mathbf{V}_{m,j} = [\mathbf{V}_{e,j}, \mathbf{V}_{t,j}], \quad (4)$$

$$\text{head}_j = \text{Softmax}\left(\frac{\mathbf{Q}_{t,j} \mathbf{K}_{m,j}}{\sqrt{D_h}}\right) \mathbf{V}_{m,j}, \quad (5)$$

where $\mathbf{Q}_{t,j} = \mathbf{H}_{t,j}^i \mathbf{W}_{q,j}$, $\mathbf{K}_{e,j} = \mathbf{H}_e \mathbf{W}_{k,j}$, and $\mathbf{K}_{t,j} = \mathbf{H}_{t,j}^i \mathbf{W}_{k,j}$, with a similar notation for $\mathbf{V}_{e,j} = \mathbf{H}_e \mathbf{W}_{v,j}$ and $\mathbf{V}_{t,j} = \mathbf{H}_{t,j}^i \mathbf{W}_{v,j}$. Concatenation is denoted by $[\cdot]$, and $\mathbf{K}_{m,j}$ and $\mathbf{V}_{m,j}$ symbolize the amalgamated features of query and key. $\mathbf{W}_{q,j}$, $\mathbf{W}_{k,j}$, and $\mathbf{W}_{v,j}$ in $\mathcal{R}^{D_h \times D_h}$ represent the projection matrices for query, key, and value for each head j , respectively. Our model’s design allows for the efficient fusion of two modalities through causal attention, facilitating conditional generation without the need for additional parameter updates to align the ECG modality. More comparisons about ECG modality alignment and other fusion approaches are illustrated in Appendix ??.

3.3 ECG Instruction Tuning

As described in Section 3.1, we have converted ECG-text pairs into a chat-bot style instruction format: $\langle \text{user} \rangle: \{\mathbf{X}_p, \mathbf{X}_e\} \langle \text{assistant} \rangle: \{\mathbf{X}_t\} \langle \text{s} \rangle$. During instruction tuning, we compute autoregressive loss only on tokens after response tokens $\langle \text{assistant} \rangle$, and use label loss masking to finetune the model, where we mask all tokens belonging to \mathbf{X}_p and \mathbf{X}_e . To save computational resources and accelerate the convergence of instruction tuning, we use LoRA [16] adapters for all linear layers of the LLM backbone \mathcal{F}_l and freeze its backbone. Subsequently, given a sequence of ECG instruction data, we compute the probability of the target response \mathbf{X}_t as an autoregressive function:

$$p(\mathbf{X}_t | \mathbf{X}_p, \mathbf{X}_e) = \prod_{i=j}^L p_\theta(\mathbf{x}_{t,i} | \mathbf{X}_p, \mathbf{X}_e, \mathbf{X}_{t,<i}), \quad (6)$$

where j is the start index after $\langle \text{assistant} \rangle$, θ is the trainable parameters of LoRA and ECG encoder \mathcal{F}_e , $\mathbf{X}_{t,<i}$ is the response tokens before the current generation $\mathbf{x}_{t,i}$.

4 Benchmarking ECG Report Generation

In this section, we create a benchmark to evaluate the ECG report generation approach. Our benchmark includes two datasets (PTB-XL and MIMIC-IV-ECG) along with three ECG-related tasks, including (1) the quality of ECG report generation, (2) the zero-shot ability under domain transfer, (3) the robustness of the model against perturbed signals.

4.1 Datasets

PTB-XL. The PTB-XL dataset [11] comprises 21,837 clinical 12-lead ECGs, each lasting 10 seconds, from 18,885 patients. Each ECG is accompanied by a corresponding report. The data includes raw ECG signals and their reports, with all recordings sampled at 500Hz over 10 seconds. We divided

this dataset into training, validation, and testing subsets in a 70%:10%:20% ratio, respectively. The human experts double-check all samples in the test set to ensure data quality. As mentioned in Sec 3.1, we reformulate the dataset into the instruction data format.

MIMIC-IV-ECG. The MIMIC-IV-ECG dataset [10] is currently the largest publicly accessible ECG dataset, containing 800,035 paired samples from 161,352 unique subjects. Similar to PTB-XL, each sample in this dataset includes a raw ECG signal and its corresponding report, with all recordings sampled at 500Hz for 10 seconds. The division of this dataset into training, validation, and testing subsets is 80%:10%:10% ratio. Likewise, we reconstruct this dataset into an ECG instruction data template.

4.2 Evaluation Metrics

We evaluate models using nine metrics: BLEU 1-4 [17], METEOR [18], ROUGE 1-2 and L [19], CIDEr-D [20], and BERTScore [21]. BLEU and METEOR assess machine translation quality, focusing on accuracy and fluency. ROUGE-L measures sentence fluency and structure, while ROUGE-1 and ROUGE-2 examine uni-gram and bi-gram overlaps. CIDEr-D evaluates the relevance and uniqueness of generated ECG reports against a candidate set, and BERTScore assesses semantic similarity to the ground truth, ensuring content accuracy.

4.3 Tasks

We evaluate the performance of ECG report generation on the following three tasks:

Quality Report Generation. This task aims to assess report quality after ECG instruction tuning using 10% of MIMIC-IV-ECG and PTB-XL datasets as the test set. The evaluation examines how closely generated reports match the original’s structure and meaning, considering various instructions and ECG inputs. We analyze metrics like BLEU-1 to 4, METEOR, ROUGE 1, 2, L, CIDEr-D, and BERTScore.

Zero-shot Generalizability. To explore the generalizability of LLMs in domain transfer scenarios following ECG instruction tuning, we trained the models on 70% of the instruction data from MIMIC-IV-ECG. Following this, we evaluated the models’ zero-shot capabilities on the PTB-XL test set. It’s important to note that the PTB-XL and MIMIC-IV-ECG datasets originate from different continents—Europe and the United States, respectively—utilizing varied devices and from distinct hospitals, across different time periods. Therefore, we consider these datasets to represent two separate domains. This distinction allows us to use the PTB-XL dataset to gauge our model’s performance in zero-shot domain transfer effectively. We used the metrics BLEU-4, METEOR, ROUGE-L, and CIDEr-D because of limited space and calculated their average for model evaluation.

Signal Perturbation Robustness. In real-world clinical settings, ECG signals often contain some degree of noise. To evaluate the robustness of MEIT against such noisy interference, we selected 10% of the ECG samples from the MIMIC-IV-ECG test dataset. We then added Gaussian noise to these samples during the models’ instruction-based inference process. For this evaluation, we used BLEU-4, METEOR, ROUGE-L, and CIDEr-D as metrics.

5 Experiments and Evaluation

5.1 Experimental Settings

In this section, we evaluate and benchmark nine open-source decoder-only LLMs using the constructed ECG report generation benchmark. Additionally, we offer a comprehensive analysis of scalability and instruction tuning and present case studies showcasing the generated reports.

Models. We use nine LLMs based on the peft³ library, which directly supports LoRA [16] to construct the multimodal ECG report generation model described in Section 3.2. These models include GPT-Neo [22], GPT-NeoX [23], GPT-J [24], BLOOM [25], OPT [26], LLaMA-1 [27], LLaMA-2 [6], Mistral [28], and Mistral-Instruct⁴, along with

³<https://github.com/huggingface/peft>

⁴<https://huggingface.co/mistralai/Mistral-7B-Instruct-v0.1>

Table 1: Natural language generation metric on MIMIC-IV-ECG. For model size, 'M' denotes the million level, and 'B' denotes the billion level. † refers to an improved instruct fine-tuned version of models. The light teal color indicates the second highest results, and heavy teal color indicates the highest results.

MODELS	SIZE	BLEU-1	BLEU-2	BLEU-3	BLEU-4	METEOR	ROUGE-L	ROUGE-1	ROUGE-2	CIDEr-D
GPT2-Medium	345M	0.576	0.527	0.456	0.425	0.551	0.523	0.544	0.512	3.70
GPT2-Large	774M	0.614	0.563	0.490	0.476	0.595	0.571	0.585	0.538	4.21
GPT-Neo	2.7B	0.631	0.579	0.534	0.489	0.727	0.689	0.715	0.592	4.81
GPT-NeoX	20B	0.645	0.588	0.539	0.523	0.719	0.701	0.712	0.622	4.92
GPT-J	6B	0.676	0.628	0.584	0.542	0.756	0.721	0.744	0.632	5.23
BLOOM	7B	0.669	0.624	0.591	0.550	0.758	0.725	0.745	0.639	5.19
OPT	6.7B	0.673	0.616	0.598	0.532	0.755	0.732	0.743	0.631	5.32
LLaMA-1	7B	0.685	0.648	0.615	0.543	0.761	0.724	0.742	0.642	5.26
Mistral	7B	0.697	0.659	0.611	0.571	0.763	0.740	0.765	0.658	5.48
LLaMA-2†	7B	0.706	0.662	0.622	0.581	0.775	0.745	0.768	0.664	5.55
Mistral-Instruct†	7B	0.714	0.665	0.619	0.576	0.768	0.751	0.762	0.667	5.62

Table 2: Natural language generation metric on PTB-XL. The light teal color indicates the second highest results, and heavy teal color indicates the highest results.

MODELS	SIZE	BLEU-1	BLEU-2	BLEU-3	BLEU-4	METEOR	ROUGE-L	ROUGE-1	ROUGE-2	CIDEr-D
GPT2-Medium	345M	0.329	0.278	0.254	0.232	0.441	0.391	0.561	0.433	2.12
GPT2-Large	774M	0.437	0.395	0.355	0.320	0.575	0.481	0.652	0.527	3.25
GPT-Neo	2.7B	0.474	0.449	0.398	0.373	0.602	0.486	0.674	0.595	3.70
GPT-NeoX	20B	0.469	0.453	0.417	0.399	0.620	0.553	0.688	0.622	3.58
GPT-J	6B	0.485	0.452	0.428	0.405	0.656	0.550	0.662	0.613	3.72
BLOOM	7B	0.491	0.462	0.427	0.415	0.665	0.580	0.678	0.605	3.80
OPT	6.7B	0.502	0.477	0.431	0.418	0.662	0.568	0.669	0.624	3.94
LLaMA-1	7B	0.514	0.485	0.465	0.430	0.678	0.588	0.682	0.613	3.97
Mistral	7B	0.486	0.475	0.446	0.421	0.673	0.591	0.697	0.634	3.98
LLaMA-2†	7B	0.515	0.484	0.469	0.439	0.675	0.594	0.698	0.624	4.05
Mistral-Instruct†	7B	0.501	0.481	0.457	0.425	0.664	0.592	0.700	0.641	4.01

two relatively small pre-trained language models (GPT2-Medium and GPT-Large [29]) as fundamental baselines.

Implementation Details. Our study utilized PyTorch 2.1, transformers [30], and accelerated on A100 GPUs with LLMs from Hugging Face [31] ranging from 2.7 to 70 billion parameters. For larger models, we used DeepSpeed⁵. The training covered 5 epochs on MIMIC-IV-ECG and PTB-XL with a 2e-5 learning rate and 64 batch size, employing a linear optimizer with a 0.03 warm-up ratio. For text preprocessing, we initially remove all instances of the 'nan' string and sentences that consist solely of numerical values. Subsequently, we discard any samples whose reports contain fewer than 5 tokens. For ECG encoder, we adopt random initialization. Additionally, the default number of generated prompts from GPT-4 is 256, more training, visualization details about ECG instruction tuning are illustrated in Appendix A.2, Section 5.3, and Appendix A.4.

Table 3: Semantic similarity between the generated ECG reports and ground truths is measured using BERTScore, denoted as P for Precision, R for Recall, and F-1 for the F-1 Score.

MODELS	MIMIC-IV-ECG			PTB-XL		
	P	R	F-1	P	R	F-1
GPT2-Medium	0.562	0.453	0.502	0.534	0.465	0.497
GPT2-Large	0.657	0.574	0.613	0.625	0.553	0.586
GPT-Neo	0.723	0.633	0.675	0.675	0.588	0.628
GPT-NeoX	0.719	0.638	0.676	0.654	0.579	0.614
GPT-J	0.725	0.655	0.688	0.689	0.622	0.654
BLOOM	0.734	0.684	0.708	0.701	0.645	0.672
OPT	0.713	0.667	0.689	0.712	0.648	0.678
LLaMA-1	0.752	0.697	0.723	0.725	0.657	0.689
Mistral	0.761	0.732	0.746	0.711	0.664	0.687
LLaMA-2†	0.764	0.725	0.744	0.721	0.668	0.693
Mistral-Instruct†	0.773	0.722	0.747	0.730	0.661	0.694

5.2 Benchmark Task Evaluation

5.2.1 Quality Evaluation

Performance on MIMIC-IV-ECG. Table 3 and 1 present the results of various types of language encoders $\mathcal{F}_l(\cdot)$ on MIMIC-IV-ECG. The results show that all LLMs perform better than smaller language models (SLMs), such as GPT2-Medium and GPT2-Large, across all evaluation metrics. Notably, from GPT-Neo to Mistral-Instruct, LLM-based backbones achieve a significant margin over SLMs in all metrics. For instance, compared to GPT2-Large, the METEOR score increases

⁵<https://github.com/microsoft/DeepSpeed>

in the range of 0.132 to 0.18 from GPT-Neo to LLaMA-2, and Mistral-Instruct outperforms GPT2-Large with an improvement of 0.18 in the ROUGE-L score and 0.134 in the F-1 of BERTScore. The observed performance underscores the adeptness of LLMs in generalizing from signal data, showcasing enhanced proficiency in aligning ECG signal representations with corresponding textual information. This highlights the significant potential of LLMs in medical signal-to-text generation. Particularly, LLaMA-2 and Mistral-Instruct surpass their counterparts in most evaluative metrics, suggesting that models pre-tuned with general instructions are more adept at learning ECG-text alignment.

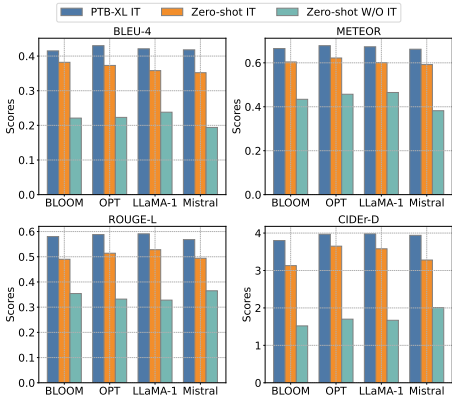


Figure 3: Zero-shot performance on PTB-XL dataset. “IT” denotes instruction tuning.

Performance on PTB-XL. As shown in Table 2, the models exhibit reduced performance on PTB-XL compared to MIMIC-IV-ECG, which is attributable to the smaller scale of the instruction data in PTB-XL. This underscores the importance of data scale in enhancing instruction-based ECG report generation. Moreover, similar to the MIMIC-IV-ECG results, all LLM-based models show significant improvement over SLMs. Specifically, LLaMA-2 surpasses GPT2-Large by 0.134 in the BLEU-3 metric, while LLaMA-1 achieves a 0.103 improvement in the METEOR score. The overall experimental results reveal that Mistral-Instruct and LLaMA-2 are consistently the top two performers across most metrics because of their strong general instruction-following capabilities.

5.2.2 Zero-shot Evaluation in Domain Transfer.

In Figure 3, we present the evaluation of the zero-shot learning capabilities of various LLMs, which is trained on the MIMIC-IV-ECG dataset and then tested on PTB-XL (unseen dataset). The assessed models include BLOOM, OPT, LLaMA-1, and Mistral. Firstly, all selected LLMs undergo instruction tuning on the MIMIC-IV-ECG train set, followed by zero-shot testing on the PTB-XL test set verified by human experts, denoted as ZERO-SHOT IT. We also measure the performance of each model in report generation without prior ECG-specific instruction tuning, denoted as ZERO-SHOT W/O IT. PTB-XL IT represents training on the PTB-XL train set and then evaluated on the PTB-XL test set. Notably, although ZERO-SHOT IT shows a slight degradation compared to PTB-XL IT, the results still indicate a variance in the model’s ability to generalize to an unseen dataset with instruction tuning (IT), compared to ZERO-SHOT W/O IT. The involvement of ECG instruction tuning on MIMIC-IV-ECG enables the models to achieve superior zero-shot performance on the unseen PTB-XL dataset, indicating the necessity of instruction tuning in enhancing the models’ zero-shot ability on unseen datasets in ECG report generation.

5.2.3 Robust Analysis with Perturbed ECG Signal.

In a noise stress evaluation [32], we added Gaussian noise to ECG signals at signal-to-noise ratios (SNRs) of 0.05, 0.1, 0.15, and 0.2 during testing to assess model robustness. Our experiments utilized four LLM architectures: BLOOM, OPT, LLaMA-1, and Mistral, each trained on clean ECG signals from the MIMIC-IV-ECG training set and tested on corresponding noise-added signals from its test set. The results, illustrated in Figure 4, show a performance decline in all LLMs as SNR decreased, highlighting the significant interference of ECG noise. Furthermore, as shown in Table 1, Mistral also excelled in tests on noise-free datasets, suggesting a synergistic effect between clean and noisy test sets. The results demonstrate Mistral’s strong resistance to perturbations. Even with more severe noise, it maintained robustness regarding ROUGE-L and METEOR metrics. Developing an even more robust framework is a goal for future research.

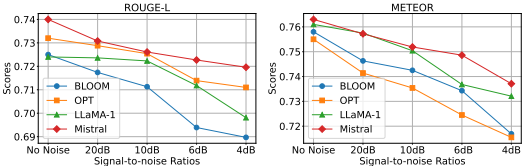


Figure 4: Signal perturbation robustness analysis on various LLMs

Table 4: Performance comparison of the proposed concatenated-fusion method and other mainstream fusion variants. We evaluate these methods on the MIMIC-IV-ECG dataset, using BLEU-4, METEOR, ROUGE-L, and CIDEr-D metrics. We take LLaMA-1 7B as the LLM backbone here. heavy teal color indicates the highest results.

FRAMEWORK	METHOD	BLEU-4	METEOR	ROUGE-L	CIDEr-D
LLaVA Flamingo	Straightforward input	0.529	0.737	0.712	4.99
	Trainable cross-attention	0.527	0.768	0.715	5.11
MEIT	Concatenated-fusion	0.543	0.761	0.724	5.26

5.3 Analysis

Instruction Tuning Visualization. Figure 5 compares the convergence curves of the instruction tuning loss and the METEOR score between GPT-Neo (2.7B), BLOOM (7B), OPT (6.7B), and LLaMA-2 (7B) on the MIMIC-IV-ECG train and validation datasets. We observe that larger models with more parameters can converge to a more minor loss and achieve higher performance on the METEOR score. Notably, an increase in model size correlates with higher performance and lower loss, suggesting that larger models have the potential for better performance.

Analysis of ECG Modality Alignment. To study the effectiveness of our proposed concatenated-fusion method for ECG modality alignment, we compare it with other fusion approaches such as direct input in LLaVA [33] and additional trainable cross-attention layer in Flamingo [12]. For straightforward input, we follow the design of LLaVA by directly concatenating the ECG encoder’s output embeddings with the sentence’s embeddings before inputting them into the LLM backbones. For the second comparison method, we follow Flamingo by adding a trainable cross-attention layer within the attention block. From Table 4, we observe that the Concatenated-fusion method outperforms the trainable cross-attention method of Flamingo in most metrics and is consistently superior to the Straightforward input method of LLaVA. Consequently, the concatenated fusion is more effective for the LLM backbone’s alignment with fine-grained ECG patterns without necessitating additional trainable parameters.

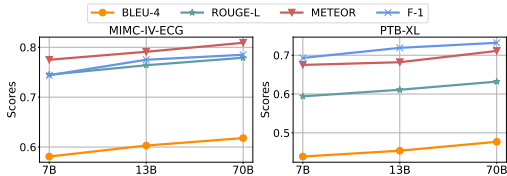
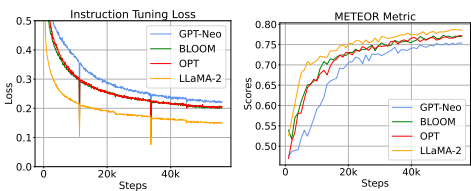


Figure 5: Instruction tuning loss and METEOR visualization. Figure 6: Model Scaling Performance on MIMIC-IV-ECG and PTB-XL.

Scalability Analysis. To investigate whether ECG instruction tuning on larger-scale models yields better results, we validated LLaMA-2 models of 7B, 13B, and 70B parameter sizes on both MIMIC-IV-ECG and PTB-XL datasets. As depicted in Figure 6, an upward trend in all evaluation metrics is observed with a gradual increase in model size.

However, it is noteworthy that the gains in performance associated with increasing model size are not particularly significant. For example, the F-1 score for the 70B model on the PTB-XL dataset exhibits a marginal increase of 0.02 over the 13B model. Similarly, on the MIMIC-IV-ECG dataset, the 70B model’s F-1 score is only 0.01 higher than that of the 13B model. Therefore, we conjecture that enhancing both data scale and model size concurrently is necessary to achieve superior performance [34].

Ablation Study on ECG Instruction Tuning. We conducted an ablation study to evaluate instruction tuning’s impact on aligning ECG signals with report representations. Utilizing LLMs such as BLOOM, OPT, LLaMA-1, and Mistral without instruction tuning, we allowed direct learning from ECG signals. The findings, illustrated in Figure 7, indicate a significant performance drop across all metrics without instruction tuning, particularly in Mistral. This underscores instruction tuning’s superiority in enhancing LLMs’ generalization to new tasks/data over direct fine-tuning [35].

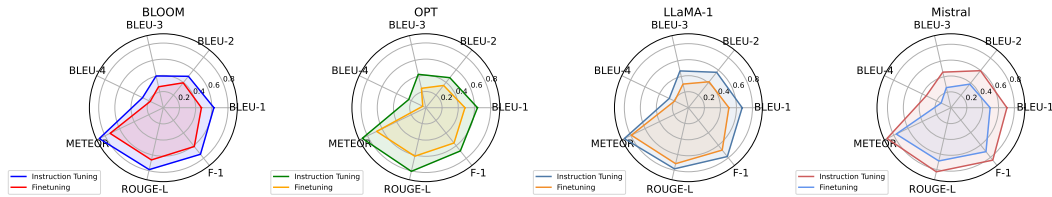


Figure 7: Ablation Study of ECG Instruction Tuning on MIMIC-IV-ECG Dataset.

Qualitative Results. In Figure 8, we randomly select two samples generated by MEIT using LLaMA-2 and Mistral-Instruct as the LLM backbones. The consistent key information, highlighted in blue, indicates that both models have successfully learned important patterns from the ECG signals. Overall, the models’ results align with the ground truth, accurately identifying cardiac abnormalities from the ECG signals. Furthermore, both models provide detailed explanations of abnormal ECG signal details, such as ‘ischemia’ from sample 1 and ‘right bundle branch block’ from sample 2. These generated reports demonstrate the efficacy of our method.

6 Related Works

Instruction Tuning. Instruction tuning [36, 37] boosts zero-shot learning in LLMs for new tasks using instructions. Notable models like InstructGPT [35], FLAN-PaLM [38], and Alpaca [39] fine-tune with instruction data through various methods, including human feedback. Similarly, multimodal models such as LLaVA [33], MiniGPT-4 [40], and AnyMAL [41] benefit from multimodal instructions for enhanced learning. However, instruction tuning for medical signals like ECG remains underexplored. Our research develops a targeted instruction-tuning framework for ECG report generation, addressing this gap.

Medical Report Generation. Medical report generation [42] involves three strategies: (1) Template Selection and Generation, highlighted by HRGR [43] and CMAS [44]; (2) Data Integration and Coherence, as seen in PPKED [45] and CA [46]; (3) Cross-Modal Alignment, with efforts like [47, 48]. While recent research has advanced these areas, applying them to ECG data is challenging due to the distinct nature of ECG signals compared to medical images.

LLM for ECG Understanding. Only a few research efforts have focused on utilizing LLMs for ECG-related tasks [49–51]. In the studies by [49, 51], the authors manually convert ECG signals into text features before feeding them into LLMs, rather than using the original ECG data. This approach overlooks the modality patterns inherent in the signals. Moreover, these studies only employ LLMs for classifying diseases from ECG data and do not explore the generation of medical reports. In contrast, [50] attempts ECG report generation by using handcrafted ECG features as inputs instead of the original signals. However, they have not publicly made any code or models available, making direct comparisons challenging.

7 Conclusion and Future Work

In this work, we propose and demonstrate the efficacy of the Multimodal ECG Instruction Tuning (MEIT) framework. Particularly, we first introduce a novel method for creating instruction-following data for ECG reports, enabling the training of an ECG report generator, a multimodal LLM designed to generate ECG reports following human instructions. Furthermore, we propose an effective and efficient method for aligning ECG and report representations across multiple open-source LLMs, achieving notable performance on both the MIMIC-IV-ECG and PTB-XL datasets for diverse tasks.

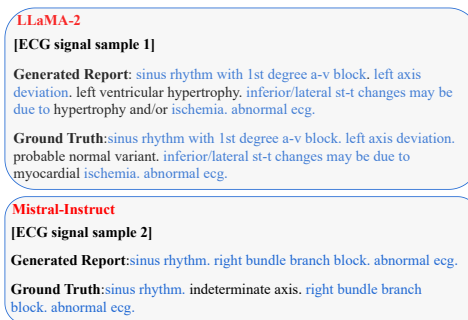


Figure 8: Examples of ECG reports generated by LLaMA-2 and Mistral-Instruct. We highlight the consistent information between the generated reports and the ground truths with blue color.

Importantly, this paper introduces the comprehensive benchmark for ECG instruction-following in ECG report generation. While this research primarily concentrates on ECG signals, it marks a preliminary step in biomedical signal instruction tuning. In future work, we plan to extend our framework to encompass additional medical signal domains, such as EEG signals, with the aspiration that our work spurs further advancements in developing more proficient medical-signal LLMs.

References

- [1] Rui Hu, Jie Chen, and Li Zhou. Spatiotemporal self-supervised representation learning from multi-lead ecg signals. *Biomedical Signal Processing and Control*, 84:104772, 2023.
- [2] Che Liu, Zhongwei Wan, Sibao Cheng, Mi Zhang, and Rossella Arcucci. Etp: Learning transferable ecg representations via ecg-text pre-training. *arXiv preprint arXiv:2309.07145*, 2023.
- [3] Che Liu, Zhongwei Wan, Cheng Ouyang, Anand Shah, Wenjia Bai, and Rossella Arcucci. Zero-shot ECG classification with multimodal learning and test-time clinical knowledge enhancement. *CoRR*, abs/2403.06659, 2024.
- [4] Zhongwei Wan. Text classification: A perspective of deep learning methods. *arXiv preprint arXiv:2309.13761*, 2023.
- [5] Josh Achiam, Steven Adler, Sandhini Agarwal, Lama Ahmad, Ilge Akkaya, Florencia Leoni Aleman, Diogo Almeida, Janko Altenschmidt, Sam Altman, Shyamal Anadkat, et al. Gpt-4 technical report. *arXiv preprint arXiv:2303.08774*, 2023.
- [6] Hugo Touvron, Louis Martin, Kevin Stone, Peter Albert, Amjad Almahairi, Yasmine Babaei, Nikolay Bashlykov, Soumya Batra, Prajjwal Bhargava, Shruti Bhosale, et al. Llama 2: Open foundation and fine-tuned chat models, 2023. URL <https://arxiv.org/abs/2307.09288>, 2023.
- [7] Zhongwei Wan, Xin Wang, Che Liu, Samiul Alam, Yu Zheng, et al. Efficient large language models: A survey. *arXiv preprint arXiv:2312.03863*, 1, 2023.
- [8] Xin Wang, Zhongwei Wan, Arvin Hekmati, Mingyu Zong, Samiul Alam, Mi Zhang, and Bhaskar Krishnamachari. Iot in the era of generative ai: Vision and challenges. *arXiv preprint arXiv:2401.01923*, 2024.
- [9] Xin Wang, Yu Zheng, Zhongwei Wan, and Mi Zhang. Svd-llm: Truncation-aware singular value decomposition for large language model compression. *arXiv preprint arXiv:2403.07378*, 2024.
- [10] Brian Gow, Tom Pollard, Larry A Nathanson, Alistair Johnson, Benjamin Moody, Chrystinne Fernandes, Nathaniel Greenbaum, Seth Berkowitz, Dana Moukheiber, Parastou Eslami, et al. MIMIC-IV-ECG-Diagnostic Electrocardiogram Matched Subset.
- [11] Patrick Wagner, Nils Strodthoff, Ralf-Dieter Boussejot, Dieter Kreiseler, Fatima I Lunze, Wojciech Samek, and Tobias Schaeffter. Ptb-xl, a large publicly available electrocardiography dataset. *Scientific data*, 7(1):154, 2020.
- [12] Jean-Baptiste Alayrac, Jeff Donahue, Pauline Luc, Antoine Miech, Iain Barr, Yana Hasson, Karel Lenc, Arthur Mensch, Katherine Millican, Malcolm Reynolds, et al. Flamingo: a visual language model for few-shot learning. *Advances in Neural Information Processing Systems*, 35: 23716–23736, 2022.
- [13] Yuhuai Wu, Markus N Rabe, DeLesley Hutchins, and Christian Szegedy. Memorizing transformers. *arXiv preprint arXiv:2203.08913*, 2022.
- [14] Zhongwei Wan, Yichun Yin, Wei Zhang, Jiabin Shi, Lifeng Shang, Guangyong Chen, Xin Jiang, and Qun Liu. G-map: general memory-augmented pre-trained language model for domain tasks. *arXiv preprint arXiv:2212.03613*, 2022.
- [15] Junnan Li, Dongxu Li, Silvio Savarese, and Steven Hoi. Blip-2: Bootstrapping language-image pre-training with frozen image encoders and large language models. *arXiv preprint arXiv:2301.12597*, 2023.

- [16] Edward J Hu, Phillip Wallis, Zeyuan Allen-Zhu, Yuanzhi Li, Shean Wang, Lu Wang, Weizhu Chen, et al. Lora: Low-rank adaptation of large language models. In *International Conference on Learning Representations*, 2021.
- [17] Kishore Papineni, Salim Roukos, Todd Ward, and Wei-Jing Zhu. Bleu: a method for automatic evaluation of machine translation. In *Proceedings of the 40th annual meeting of the Association for Computational Linguistics*, pages 311–318, 2002.
- [18] Satanjeev Banerjee and Alon Lavie. Meteor: An automatic metric for mt evaluation with improved correlation with human judgments. In *Proceedings of the acl workshop on intrinsic and extrinsic evaluation measures for machine translation and/or summarization*, pages 65–72, 2005.
- [19] Chin-Yew Lin. Rouge: A package for automatic evaluation of summaries. In *Text summarization branches out*, pages 74–81, 2004.
- [20] Ramakrishna Vedantam, C Lawrence Zitnick, and Devi Parikh. Cider: Consensus-based image description evaluation. In *Proceedings of the IEEE conference on computer vision and pattern recognition*, pages 4566–4575, 2015.
- [21] Tianyi Zhang, Varsha Kishore, Felix Wu, Kilian Q Weinberger, and Yoav Artzi. Bertscore: Evaluating text generation with bert. *arXiv preprint arXiv:1904.09675*, 2019.
- [22] Sid Black, Leo Gao, Phil Wang, Connor Leahy, and Stella Biderman. GPT-Neo: Large Scale Autoregressive Language Modeling with Mesh-Tensorflow, March 2021. URL <https://doi.org/10.5281/zenodo.5297715>. If you use this software, please cite it using these metadata.
- [23] Sid Black, Stella Biderman, Eric Hallahan, Quentin Anthony, Leo Gao, Laurence Golding, Horace He, Connor Leahy, Kyle McDonell, Jason Phang, et al. Gpt-neox-20b: An open-source autoregressive language model. *arXiv preprint arXiv:2204.06745*, 2022.
- [24] Ben Wang and Aran Komatsuzaki. GPT-J-6B: A 6 Billion Parameter Autoregressive Language Model. <https://github.com/kingoflolz/mesh-transformer-jax>, May 2021.
- [25] BigScience Workshop, Teven Le Scao, Angela Fan, Christopher Akiki, Ellie Pavlick, Suzana Ilić, Daniel Hesslow, Roman Castagné, Alexandra Sasha Luccioni, François Yvon, et al. Bloom: A 176b-parameter open-access multilingual language model. *arXiv preprint arXiv:2211.05100*, 2022.
- [26] Susan Zhang, Stephen Roller, Naman Goyal, Mikel Artetxe, Moya Chen, Shuohui Chen, Christopher Dewan, Mona Diab, Xian Li, Xi Victoria Lin, et al. Opt: Open pre-trained transformer language models. *arXiv preprint arXiv:2205.01068*, 2022.
- [27] Hugo Touvron, Thibaut Lavril, Gautier Izacard, Xavier Martinet, Marie-Anne Lachaux, Timothée Lacroix, Baptiste Rozière, Naman Goyal, Eric Hambro, Faisal Azhar, Aurélien Rodriguez, Armand Joulin, Edouard Grave, and Guillaume Lample. Llama: Open and efficient foundation language models. *CoRR*, abs/2302.13971, 2023.
- [28] Albert Q Jiang, Alexandre Sablayrolles, Arthur Mensch, Chris Bamford, Devendra Singh Chaplot, Diego de las Casas, Florian Bressand, Gianna Lengyel, Guillaume Lample, Lucile Saulnier, et al. Mistral 7b. *arXiv preprint arXiv:2310.06825*, 2023.
- [29] Alec Radford, Jeffrey Wu, Rewon Child, David Luan, Dario Amodei, Ilya Sutskever, et al. Language models are unsupervised multitask learners. *OpenAI blog*, 1(8):9, 2019.
- [30] Thomas Wolf, Lysandre Debut, Victor Sanh, Julien Chaumond, Clement Delangue, Anthony Moi, Pierric Cistac, Tim Rault, Rémi Louf, Morgan Funtowicz, Joe Davison, Sam Shleifer, Patrick von Platen, Clara Ma, Yacine Jernite, Julien Plu, Canwen Xu, Teven Le Scao, Sylvain Gugger, Mariama Drame, Quentin Lhoest, and Alexander M. Rush. Transformers: State-of-the-art natural language processing. In *Proceedings of the 2020 Conference on Empirical Methods in Natural Language Processing: System Demonstrations*, pages 38–45, Online, October 2020. Association for Computational Linguistics. URL <https://www.aclweb.org/anthology/2020.emnlp-demos.6>.

- [31] Thomas Wolf, Lysandre Debut, Victor Sanh, Julien Chaumond, Clement Delangue, Anthony Moi, Pierric Cistac, Tim Rault, Rémi Louf, Morgan Funtowicz, et al. Huggingface’s transformers: State-of-the-art natural language processing. *arXiv preprint arXiv:1910.03771*, 2019.
- [32] Jilong Wang, Renfa Li, Rui Li, Keqin Li, Haibo Zeng, Guoqi Xie, and Li Liu. Adversarial de-noising of electrocardiogram. *Neurocomputing*, 349:212–224, 2019.
- [33] Haotian Liu, Chunyuan Li, Qingyang Wu, and Yong Jae Lee. Visual instruction tuning. *arXiv preprint arXiv:2304.08485*, 2023.
- [34] Jason Wei, Yi Tay, Rishi Bommasani, Colin Raffel, Barret Zoph, Sebastian Borgeaud, Dani Yogatama, Maarten Bosma, Denny Zhou, Donald Metzler, et al. Emergent abilities of large language models. *arXiv preprint arXiv:2206.07682*, 2022.
- [35] Long Ouyang, Jeffrey Wu, Xu Jiang, Diogo Almeida, Carroll Wainwright, Pamela Mishkin, Chong Zhang, Sandhini Agarwal, Katarina Slama, Alex Ray, et al. Training language models to follow instructions with human feedback. *Advances in Neural Information Processing Systems*, 35:27730–27744, 2022.
- [36] Shengyu Zhang, Linfeng Dong, Xiaoya Li, Sen Zhang, Xiaofei Sun, Shuhe Wang, Jiwei Li, Runyi Hu, Tianwei Zhang, Fei Wu, et al. Instruction tuning for large language models: A survey. *arXiv preprint arXiv:2308.10792*, 2023.
- [37] Yizhong Wang, Hamish Ivison, Pradeep Dasigi, Jack Hessel, Tushar Khot, Khyathi Raghavi Chandu, David Wadden, Kelsey MacMillan, Noah A Smith, Iz Beltagy, et al. How far can camels go? exploring the state of instruction tuning on open resources. *arXiv preprint arXiv:2306.04751*, 2023.
- [38] Hyung Won Chung, Le Hou, Shayne Longpre, Barret Zoph, Yi Tay, William Fedus, Yunxuan Li, Xuezhi Wang, Mostafa Dehghani, Siddhartha Brahma, et al. Scaling instruction-finetuned language models. *arXiv preprint arXiv:2210.11416*, 2022.
- [39] Rohan Taori, Ishaan Gulrajani, Tianyi Zhang, Yann Dubois, Xuechen Li, Carlos Guestrin, Percy Liang, and Tatsunori B Hashimoto. Alpaca: A strong, replicable instruction-following model. *Stanford Center for Research on Foundation Models*. <https://crfm.stanford.edu/2023/03/13/alpaca.html>, 3(6):7, 2023.
- [40] Deyao Zhu, Jun Chen, Xiaoqian Shen, Xiang Li, and Mohamed Elhoseiny. Minigpt-4: Enhancing vision-language understanding with advanced large language models. *arXiv preprint arXiv:2304.10592*, 2023.
- [41] Seungwhan Moon, Andrea Madotto, Zhaojiang Lin, Tushar Nagarajan, Matt Smith, Shashank Jain, Chun-Fu Yeh, Prakash Murugesan, Peyman Heidari, Yue Liu, et al. Anymal: An efficient and scalable any-modality augmented language model. *arXiv preprint arXiv:2309.16058*, 2023.
- [42] Che Liu, Zhongwei Wan, Yuqi Wang, Hui Shen, Haozhe Wang, Kangyu Zheng, Mi Zhang, and Rossella Arcucci. Benchmarking and boosting radiology report generation for 3d high-resolution medical images. *arXiv e-prints*, pages arXiv–2406, 2024.
- [43] Yuan Li, Xiaodan Liang, Zhiting Hu, and Eric P Xing. Hybrid retrieval-generation reinforced agent for medical image report generation. *Advances in neural information processing systems*, 31, 2018.
- [44] Baoyu Jing, Pengtao Xie, and Eric Xing. On the automatic generation of medical imaging reports. *arXiv preprint arXiv:1711.08195*, 2017.
- [45] Fenglin Liu, Xian Wu, Shen Ge, Wei Fan, and Yuexian Zou. Exploring and distilling posterior and prior knowledge for radiology report generation. In *Proceedings of the IEEE/CVF conference on computer vision and pattern recognition*, pages 13753–13762, 2021.
- [46] Xuwei Ma, Fenglin Liu, Changchang Yin, Xian Wu, Shen Ge, Yuexian Zou, Ping Zhang, and Xu Sun. Contrastive attention for automatic chest x-ray report generation. *arXiv preprint arXiv:2106.06965*, 2021.

- [47] Zhihong Chen, Yaling Shen, Yan Song, and Xiang Wan. Cross-modal memory networks for radiology report generation. *arXiv preprint arXiv:2204.13258*, 2022.
- [48] Han Qin and Yan Song. Reinforced cross-modal alignment for radiology report generation. In *Findings of the Association for Computational Linguistics: ACL 2022*, pages 448–458, 2022.
- [49] Chunyu Liu, Yongpei Ma, Kavitha Kothur, Armin Nikpour, and Omid Kavehei. Biosignal copilot: Leveraging the power of llms in drafting reports for biomedical signals. *medRxiv*, pages 2023–06, 2023.
- [50] Jielin Qiu, William Han, Jiacheng Zhu, Mengdi Xu, Michael Rosenberg, Emerson Liu, Douglas Weber, and Ding Zhao. Transfer knowledge from natural language to electrocardiography: Can we detect cardiovascular disease through language models? In *Findings of the Association for Computational Linguistics: EACL 2023*, pages 442–453, 2023.
- [51] Han Yu, Peikun Guo, and Akane Sano. Zero-shot ecg diagnosis with large language models and retrieval-augmented generation. In *Machine Learning for Health (ML4H)*, pages 650–663. PMLR, 2023.
- [52] Jing Xiong, Zhongwei Wan, Xiping Hu, Min Yang, and Chengming Li. Self-consistent reasoning for solving math word problems. *arXiv preprint arXiv:2210.15373*, 2022.
- [53] Zhenyu Liang, Yunfan Li, and Zhongwei Wan. Large scale many-objective optimization driven by distributional adversarial networks. *arXiv preprint arXiv:2003.07013*, 2020.
- [54] Zhenyu Liang, Yunfan Li, and Zhongwei Wan. Many-objective estimation of distribution optimization algorithm based on wgan-gp. *arXiv preprint arXiv:2003.08295*, 2020.
- [55] Kangyu Zheng, Yingzhou Lu, Zaixi Zhang, Zhongwei Wan, Yao Ma, Marinka Zitnik, and Tianfan Fu. Structure-based drug design benchmark: Do 3d methods really dominate? *arXiv e-prints*, pages arXiv–2406, 2024.
- [56] Alec Radford, Jong Wook Kim, Chris Hallacy, Aditya Ramesh, Gabriel Goh, Sandhini Agarwal, Girish Sastry, Amanda Askell, Pamela Mishkin, Jack Clark, et al. Learning transferable visual models from natural language supervision. In *International conference on machine learning*, pages 8748–8763. PMLR, 2021.
- [57] Zhongwei Wan, Che Liu, Mi Zhang, Jie Fu, Benyou Wang, Sibio Cheng, Lei Ma, César Quilodrán-Casas, and Rossella Arcucci. Med-unic: Unifying cross-lingual medical vision-language pre-training by diminishing bias. *Advances in Neural Information Processing Systems*, 36, 2024.

A Appendix.

A.1 Limitations and Future Work

In this work, we propose an effective and efficient method for generating ECG reports. Since this is a generative task, the content produced may occasionally lead to hallucinations. This is particularly pertinent in medical contexts such as ECG report generation, where accuracy is of utmost importance. To mitigate this issue, future iterations of our work could incorporate retrieval-augmented methods [14], information optimized strategies [52–54]. For instance, by integrating a retrieval mechanism that accesses a database of verified medical or biological knowledge [55] or previous ECG reports, the model could be guided towards generating more accurate and reliable outputs.

A.2 Hyper-parameters of ECG Instruction Tuning

Table 5: Hyper-parameters of ECG instruction tuning for all LLM backbones. Table 6: ECG dimension of different language models.

Hyperparameters		MODELS	ECG Dimension
Mixed precision	bf16	GPT2-Medium	64
Instruction tuning epochs	5	GPT2-Large	64
LoRA alpha	64	GPT-Neo	128
LoRA rank	128	GPT-NeoX	96
LoRA dropout	0.1	GPT-J	256
Total batch size	64	BLOOM	128
Gradient accumulation	2	OPT	128
Maximum sequence length	256	LLaMA-1	128
Learning rate	2e-5, 1e-4	Mistral	128
Learning rate Optimizer	AdamW	LLaMA-2	128
Schedule	linear	Mistral-Instruct	128
Warm-up ratio	0.03		
Weight decay	0.0		

In this study, we implement the Low-Rank Adaptation (LoRA) [16] technique for efficient fine-tuning, specifically applied to ECG instruction tuning. As detailed in Table 5 provided, we utilize mixed precision at bf16 for enhanced computational efficiency. Our models undergo instruction tuning over 5 epochs, with LoRA parameters set at an alpha of 64 and a rank of 128, accompanied by a dropout rate of 0.1. The total batch size is 64, with a gradient accumulation factor of 2. The maximum sequence length is constrained to 256 tokens. Additionally, we adopt a learning rate with 2e-5 for GPT-NeoX and 1e-4 for the other models, optimized using the AdamW algorithm. The learning rate follows a linear schedule with a warm-up ratio of 0.03. We set the weight decay to 0.0.

Moreover, as shown in Table 6, we detail the ECG embedding dimensions for various language models, highlighting their approach to ECG data encoding. GPT2-Medium and GPT2-Large feature ECG dimensions 64, while GPT-Neo, BLOOM, OPT, LLaMA-1, Mistral, LLaMA-2, and Mistral-Instruct use a dimension of 128. GPT-NeoX employs a dimension of 96, and GPT-J notably uses the largest dimension of 256. These dimensions, reflecting each model’s head dimension design, illustrate diverse strategies in ECG data processing across different models.

A.3 More Details of ECG Encoder

Projection Layer For the design of the projection layer within the ECG encoder, we adopt a non-linear approach similar to CLIP [56] and Med-UniC [57]. Specifically, in our experiments, we employ two consecutive linear layers, each followed by BatchNorm1d⁶. Besides, ReLU serves as the activation function between the two linear layers. The default settings for input and hidden layers dimensions are set to 2048 in our experiment.

⁶<https://pytorch.org/docs/stable/generated/torch.nn.BatchNorm1d.html>

Table 7: Parameter Comparison of ECG encoder and LLM backbone. We use LLaMA-1 7B as an example.

MODULE	Trainable Params	Inference Params
LLM backbone	159M	6.90B
ECG encoder	20.4M	20.4M

Parameter Size Analysis To demonstrate the ECG encoder’s lightweight design, we analyzed its trainable parameters during instruction tuning and total parameters during inference, using the LLaMA-1 7B model for illustration (Table 7). The analysis reveals the ECG encoder’s trainable parameters are substantially fewer than those of the LoRA adapter in the LLM backbone during instruction tuning, and its parameter share of the overall framework is minimal for inference, underscoring its efficiency.

A.4 Further Analysis of Generated Prompts

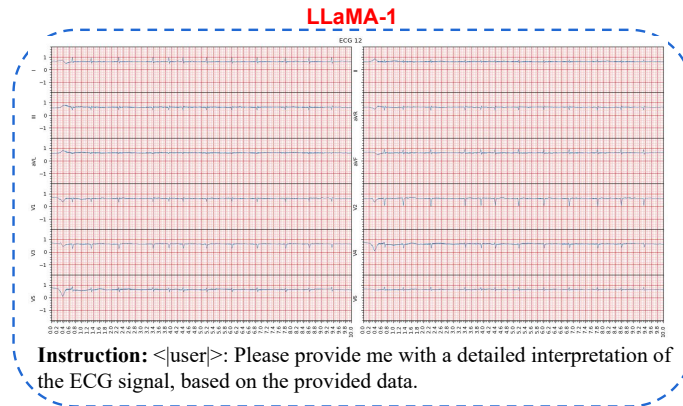
In the ECG instruction data curation, we manually created 32 prompt examples, as illustrated in Section 3.1. To increase the diversity of our samples, we employed GPT-4 to rephrase these manually designed prompts, generating a larger pool of prompt examples. These generated examples were randomly sampled and paired with ECG-text pairs to compile the ECG instruction dataset. In this section, We compare the experiment’s effects using 128, 256, and 512-generated samples, respectively. Table 8 shows the corresponding results with different dimensions. When the number is 256, it can achieve better results in most experimental settings. Hence, we take 256 generated samples as our default setting during the instruction tuning and inference.

Table 8: Performance comparison of different numbers of generated prompt samples. We evaluate them on the MIMIC-IV-ECG dataset, using BLEU-4, METEOR, ROUGE-L, and CIDEr-D metrics. We take LLaMA-1 7B as the LLM backbone here. **heavy teal** color indicates the highest results.

PROMPT NUMS	BLEU-4	METEOR	ROUGE-L	CIDEr-D
128	0.541	0.756	0.718	5.15
256	0.543	0.761	0.724	5.26
512	0.538	0.754	0.732	5.03

A.5 Visualization of Generated ECG Report Samples

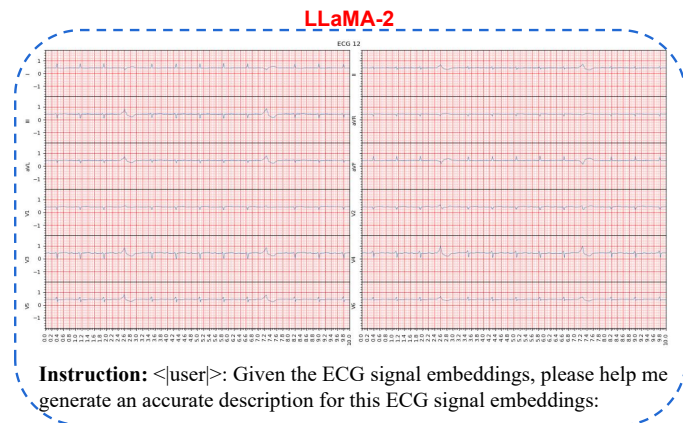
As illustrated in Figures 9, 10, and 11 we have visualized the report samples generated by LLaMA-1, LLaMA-2, and Mistral-Instruct. The samples are presented in **blue** font to highlight the key information that aligns with the ground truth. The visualization demonstrates that all three selected models can capture the essential patterns of ECG signals and generate accurate reports. This underscores the efficacy of our proposed **MEIT** framework, which is adaptable to most open-source LLMs. It effectively learns the correct clinical semantics of ECG signals, thereby enabling the generation of corresponding reports.



Generated Report: <assistant>: atrial fibrillation. extensive st-t changes may be due to myocardial ischemia. abnormal ecg.</s>

Ground Truth: <assistant>: atrial fibrillation. possible inferior infarct - age undetermined. possible anteroseptal infarct - age undetermined. lateral st-t changes may be due to myocardial ischemia. abnormal ecg.</s>

Figure 9: Reports generated by LLaMA-1 following ECG instruction Tuning.

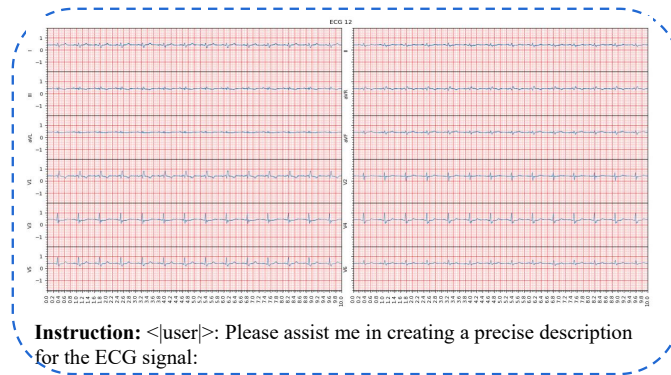


Generated Report: <assistant>: sinus rhythm with 1st degree a-v block. left axis deviation. left ventricular hypertrophy. inferior/lateral st-t changes may be due to hypertrophy and/or ischemia. abnormal ecg. </s>

Ground Truth: <assistant>: sinus rhythm with 1st degree a-v block. left axis deviation. probable normal variant. inferior/lateral st-t changes may be due to myocardial ischemia. abnormal ecg. </s>

Figure 10: Reports generated by LLaMA-2 following ECG instruction Tuning.

Mistral-Instruct



Generated Report: <|assistant|>: sinus rhythm. right bundle branch block. abnormal ecg.</s>

Ground Truth: <|assistant|>: sinus rhythm. indeterminate axis. right bundle branch block. abnormal ecg. </s>

Figure 11: Reports generated by Mistral-Instruct following ECG instruction Tuning.